Vision, Modeling, and Visualization (2012)
M. Goesele, T. Grosch, B. Preim, H. Theisel, and K. Toennies (Eds.)

Cyclic Numerical Time Integration in Variational Non-Rigid Image Registration based on Quadratic Regularisation

A. Mang[1], T. A. Schuetz[1,2], S. Becker[1,3], A. Toma[1,3] & T. M. Buzug[†1]

[1]Institute of Medical Engineering, University of Lübeck, Germany
[2]Graduate School for Computing in Medicine and Life Sciences, University of Lübeck
[3]Centre of Excellence for Technology and Engineering in Medicine (TANDEM), Lübeck, Germany

Abstract

In the present work, a novel computational framework for variational non-rigid image registration is discussed. The fundamental aim is to provide an alternative to approximate approaches based on successive convolution, which have gained great popularity in recent years, due to their linear complexity and ease of implementation.
An optimise-then-discretise *framework is considered. The corresponding* Euler-Lagrange *equations (ELEs), which arise from calculus of variation, constitute a necessary condition for a minimiser of the variational optimisation problem. The conventional, semi-implicit (SI) time integration for the solution of the ELEs is replaced by an explicit approach rendering the implementation straightforward. Since explicit methods are subject to a restrictive stability requirement on the maximal admissible time step size, they are in general inefficient and prone to get stuck in local minima. As a remedy, we take advantage of methods based on cyclic explicit numerical time integration. With this the strong stability requirement on each individual time step can be replaced by a relaxed stability requirement. This in turn results in an unconditionally stable method, which is as efficient as SI approaches.*
As a basis of comparison, SI methods are considered. Generalisability is demonstrated within a generic variational framework based on quadratic regularisation. Qualitative and quantitative analysis of numerical experiments based on synthetic test data demonstrates accuracy and efficiency.

Categories and Subject Descriptors (according to ACM CCS): I.4 [Image Processing and Computer Vision]: Enhancement—Registration

1. Introduction

Non-rigid image registration [HHH01,CHH04,FM08,SP12] is a versatile and powerful tool in medical image computing with a variety of different applications. It is about establishing spatial correspondence between two or more views of the same object, acquired from different fields of vision by different imaging sensors (multi-modal) or at different points in time (multi-temporal, serial). More precisely, the task is, given two images, a template image, T, and a reference image, R, find a *plausible* mapping, $y \in \mathcal{Y} \subset \{\tilde{y} : \mathbf{R}^d \to \mathbf{R}^d\}$, such that $T \circ y = R$ [Mod04, FM08]. Here, $d \in \{2,3\}$ is the dimensionality. The search for a suitable function, y, is typically phrased as a variational optimisation problem. At this, the distance between T and R is measured in terms of some functional, $\mathcal{D}$. However, minimising solely $\mathcal{D}$ is an ill-posed problem. One remedy to ensure well-posedness is to add a regulariser, $\mathcal{R}$, to the objective to form a joint objective functional, $\mathcal{J}$.

Different regularisation models, $\mathcal{R}$, have been designed in recent years. They are in general motivated from continuum theory and determine requirements on the smoothness and/or regularity of the mapping, y. Popular approaches include (hyper-)elastic [Bro81,Chr96,DHLH11], fluid [Chr96, CTH05, BNG96], curvature (bi-harmonic) [FM03, Hen05], total variation [CC11] or diffusion [FM02, Thi98] regularisation. The particular choice of $\mathcal{R}$ in general depends on the area of application. In addition, different soft or hard constraints have been proposed as an additional ingredient to rule out undesirable (irregular) solutions from

† Send correspondence to {mang,buzug}@imt.uni-luebeck.de.

DOI: 10.2312/PE/VMV/VMV12/143-150

the search space, or, likewise, privilege a particular solution [HM04, PMS10].

For computing a minimiser of the joint objective functional, $\mathcal{J}$, one can in general distinguish between two frameworks: *discretise-then-optimise* (DO; cf. e.g. [Mod09]) and *optimise-then-discretise* (OD; cf. e.g. [Mod04]). In the former, the optimisation problem is discretised directly. The 2$^{\text{nd}}$, traditional approach, which is considered here, is based on calculus of variation: The GÂTEAUX derivative of $\mathcal{J}$ yields a necessary condition for a minimiser. The resulting Euler-Lagrange equations (ELEs) constitute a system of differential equations, which has to be discretised and solved numerically.

Different approaches have been designed in recent years in order to compute a solution to the ELEs, most of which have been tailored to a specific type of regulariser, $\mathcal{R}$, in combination with adequate boundary conditions (e.g. fluid regularisation with periodic boundary conditions [CTH05, BNG96] or diffusion [FM02] and curvature regularisation [FM03] with homogeneous NEUMANN boundary conditions). In early work on variational non-rigid image registration (see e.g. [CRM96]) conventional iterative solvers have been used. The fundamental problem is their low asymptotic speed of convergence. Faster approaches have been developed in recent years including multigrid [CTH05, Hen05, CC11, FSHW08], additive operator-splitting (AOS) [Mod04, FM02] and FOURIER techniques [Mod04, CNH07, LRVMMS08] as well as convolution based methods [BNG96, Thi98, VPPA08, VPPA09, CNH09, CNH10, BKF10]. The latter have become very popular, due to their ease of implementation and their linear computational complexity. The general idea of these approaches is to approximate the regulariser by projecting the solution onto a smooth space via successive convolution with some suitable kernel. From a theoretical perspective, this approximate framework is based on strong assumptions, which are in general not fulfilled and—from a practical point of view—it is less accurate than other available strategies based on numerical differentiation [Mod04].

The present work aims at designing a numerical framework, which closes the gap between efficient, approximate models that feature a low implementation complexity [BNG96, Thi98, VPPA08, VPPA09, CNH09, CNH10, BKF10] and sophisticated numerical methods [CRM96, CTH05, Hen05, CC11, FSHW08, Mod04, FM02, Mod04, CNH07, LRVMMS08], which provide greater accuracy. It turns out that there readily exists such a framework [Gen79, GS78, AAG96, GWB10], which is based on cyclic, explicit numerical time integration. The fundamental contribution of the present work is to introduce these approaches to variational, non-rigid image registration. Generalisability is demonstrated by testing the methodology within a generic L^2-norm based regularisation framework. More precisely, results are provided for diffusion [FM02], curvature [FM03], elastic [Bro81, Chr96] and 2$^{\text{nd}}$ order elastic [CNH10] regularisation. As a basis of comparison conventional SI numerical time integration is considered, too.

2. Methodology and Theory

2.1. General Mathematical Model

We treat non-rigid image registration as a variational optimisation problem. At this, images are modelled as compactly supported, continuous functions, $T, R \in \mathcal{I} \subset \{I : \mathbf{R}^d \supset \Omega \to \mathbf{R}\}$, defined on a d-dimensional interval $\Omega := (\omega_1^1, \omega_2^1) \times \cdots \times (\omega_1^d, \omega_2^d) \subset \mathbf{R}^d$, with boundary, $\partial\Omega$. The task of image registration is to find a *suitable* spatial mapping, $y = (y^1, \ldots, y^d) \in \mathcal{Y}$, $y = x - u(x)$, where $u = (u^1, \ldots, u^d) \in \mathbf{R}^d$ denotes a displacement vector, such that—ideally—$T \circ y = R$ (cf. e.g. [Mod04, FM08]). To compute y we formulate the registration problem within a TIKHONOV-regularisation framework:

$$\min_y \{\mathcal{J}(R,T;y) = \mathcal{D}(R,T;y) + \alpha\mathcal{R}(y - y_r)\}. \quad (1)$$

Here, $\mathcal{D} : \mathcal{I} \times \mathcal{I} \times \mathcal{Y} \to \mathbf{R}$ measures the distance between T and R and $\mathcal{R} : \mathcal{Y} \to \mathbf{R}$ is a regulariser, which prescribes properties of an adequate mapping, y. Further, y_r is a reference mapping, which allows for introducing prior knowledge into the regularisation model. In general, we have $y_r \equiv x$.

2.2. Distance Measure

As for the distance measure, $\mathcal{D}$, we assume—without loss of generality—that $R \approx T \circ y$. Thus, the L^2-distance

$$\mathcal{D}(R,T;y) = \frac{1}{2}\int_\Omega (T(x - u(x)) - R(x))^2 \mathrm{d}x \quad (2)$$

between T and R is a valid option. Other measures, $\mathcal{D}$, that are less strict in terms of the intensity relationship can e.g. be found in [Mod04, HHH01]. As we consider an OD framework here, the GÂTEAUX derivative of $\mathcal{D}$ has to be computed. Thus, let $T \in C^2(\Omega)$, $R \in L^2(\Omega)$, $u \in L^2(\Omega)^d$ and some pertubation $v \in L^2(\Omega)^d$ be given. The GÂTEAUX derivative of $\mathcal{D}$ with respect to v is given by (cf. e.g. [Mod04])

$$\mathrm{d}_{u;v}\mathcal{D}(R,T;u) = \int_\Omega \langle b(x,T,R,u(x)), v(x)\rangle_{\mathbf{R}^d}\,\mathrm{d}x; \quad (3)$$

$b(x,T,R,u(x)) = -(T(x - u(x)) - R(x))\nabla T(x - u(x))$ is a force field, which drives the registration; $\nabla := (\partial_{x^1}, \ldots, \partial_{x^d})^\mathsf{T} \in \mathbf{R}^d$, where ∂_{x^i} represents the partial derivative along the i-th spatial direction.

2.3. Quadratic Regularisers

As has already been discussed in §1 there exist a variety of different regularisation models [Bro81, Chr96, DHLH11, Chr96, CTH05, BNG96, FM02, Thi98, FM03, Hen05, CC11].

In the present work we limit ourselves to quadratic regularisation. At this, $\mathcal{R}$ can compactly be represented via

$$\mathcal{R}(u) = \frac{1}{2}\int_\Omega \langle \mathcal{B}[u], \mathcal{B}[u]\rangle \mathrm{d}x. \tag{4}$$

Here, $\mathcal{B}$, is some differential operator. In general format, the GÂTEAUX derivative of (4) reads

$$\mathrm{d}_{u,v}\mathcal{R}(u) = \int_\Omega \langle \mathcal{A}[u](x), v(x)\rangle_{\mathbf{R}^d} \mathrm{d}x, \tag{5}$$

where $\mathcal{A}$ is a differential operator subject to appropriate boundary conditions.

In the present manuscript we consider three prominent regularisation models, namely diffusion [FM02], curvature [FM03] and elastic regularisation (of first [Bro81, Chr96] and 2nd order [CNH10]). The individual models read

$$\mathcal{R}_D(u) = \frac{1}{2}\sum_{i=1}^{d}\int_\Omega \langle \nabla u^i, \nabla u^i\rangle \mathrm{d}x \tag{6}$$

for diffusion regularisation,

$$\mathcal{R}_C(u) = \frac{1}{2}\sum_{i=1}^{d}\int_\Omega (\Delta u^i)^2 \mathrm{d}x, \tag{7}$$

for curvature regularisation and

$$\mathcal{R}_E(u) = \frac{1}{2}\int_\Omega \left(\frac{\mu}{2}\sum_{i,j=1}^{d}(\partial_{x^i}u^j + \partial_{x^j}u^i)^2 + \lambda(\nabla\cdot u)^2\right)\mathrm{d}x, \tag{8}$$

and

$$\mathcal{R}_{E2}(u) = \frac{1}{2}\int_\Omega \left(\frac{\mu}{3}\Sigma(u) + \lambda\|\nabla(\nabla\cdot u)\|_2^2\right)\mathrm{d}x, \tag{9}$$

where

$$\Sigma(u) = \sum_{i=1}^{d}\sum_{j=1}^{d}\sum_{k=1}^{d}\left(\partial^2_{x^ix^j}u^k + \partial^2_{x^ix^k}u^j + \partial^2_{x^jx^k}u^i\right)^2$$

for elastic regularisation of 1st and 2nd order, respectively. The differential operators that result from the GÂTEAUX derivative of (6)-(9) are given by

$$\mathcal{A}_D[u] = -\Delta u, \tag{10}$$
$$\mathcal{A}_C[u] = \Delta^2 u, \tag{11}$$
$$\mathcal{A}_E[u] = -\mu\Delta u - (\lambda+\mu)\nabla(\nabla\cdot u), \tag{12}$$
$$\mathcal{A}_{E2}[u] = \mu\Delta^2 u + (\lambda+2\mu)\Delta\nabla(\nabla\cdot u). \tag{13}$$

Each of these regularisers has distinct features, which makes them particularly suited for a given application. The diffusion regularisation decouples with respect to the individual spatial directions. Curvature regularisation is immune against missing pre-registration. Elastic regularisation is physically motivated, which makes it in particular interesting for medical imaging applications. The second order elastic regulariser combines the features of curvature and elastic regularisation: it couples the regularisation along the spatial directions and comprises affine mappings in its kernel. To illustrate the properties an impulse response with respect to the individual differential operators, $\mathcal{A}$, is displayed in Fig. 1.

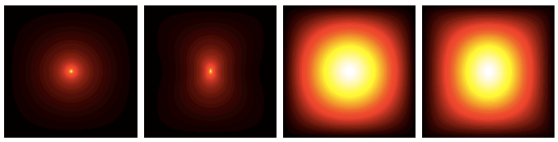

Figure 1: *Impulse response for the considered regularisation models (from left to right: diffusion, elastic, curvature and 2nd order elastic regularisation).*

3. Numerical Solution

3.1. Continuous Mathematical Model

As has been stated in the beginning of this manuscript, we consider an OD framework. Thus, the computation of a minimiser of (1) translates into computing a solution of the ELE

$$\alpha\mathcal{A}[u](x) = b(x,T,R,u) \quad \text{on } \Omega, \tag{14a}$$
$$\mathcal{B}_{BC}u(x) = 0 \quad \text{on } \partial\Omega, \tag{14b}$$

where $\mathcal{B}_{BC}$ is some suitable boundary condition. The force vector, b, and the operator, $\mathcal{A}$, in (14a) are the GÂTEAUX derivatives of $\mathcal{D}$ (see (3)) and $\mathcal{R}$ (see (10)-(13)), respectively.

A solution to (14) can be obtained by a fixed point iteration. However, this is delicate since $\mathcal{A}$ may have a non-trivial kernel. A common strategy to stabilise (14) is to introduce an artificial time variable, $t > 0$ [Mod04]. One obtains

$$\partial_t u(x,t) + \alpha\mathcal{A}[u](x,t) = b(x,t,T,R,u) \quad \text{on } \Omega\times\mathbf{R}^+, \tag{15a}$$
$$\mathcal{B}_{BC}u(x,t) = 0 \quad \text{on } \partial\Omega\times\mathbf{R}^+, \tag{15b}$$
$$u(x,t) = u_0 \quad \text{on } \Omega\times\{0\}. \tag{15c}$$

3.2. Discretisation

A cell-centred grid, $\Omega^h \in \mathbf{R}^{dm^1\times\cdots\times m^d}$, $m^i \in \mathbf{N}, i = 1,\ldots,d$, is used for discretisation. At this, the grid coordinates, $x_k := (x_k^1,\ldots,x_k^d)^\mathsf{T} \in \mathbf{R}^d$, $k \in \mathbf{Z}^d$, with $x_k^i = \omega_1^i + (h^i - 0.5)k^i$, $i = 1,\ldots,d$, represent the centre point of a cell of width $h = (h^1,\ldots,h^d) \in \mathbf{R}^d$, $h^i = (\omega_2^i - \omega_1^i)/m^i$. Further, the time axis is discretised via $t^j := jh_t$, $h_t > 0$, $j = 0,\ldots,m_t$.

In order to develop a compact matrix-vector framework, the displacement vectors, $\tilde{u}(x_k,t^j) =: u_k^j \in \mathbf{R}^d$ and the grid points, $x_k \in \mathbf{R}^d$, are assembled in a lexicographical ordering, $\omega^h = (x_k) \in \mathbf{R}^{n_d}$, $n_d = d\prod_{i=1}^d m^i$, and, $u^{h,j} = (u_k^j) \in \mathbf{R}^{n_d}$, respectively. Further, we assemble the discrete images in vector format, $T^h, R^h : \omega^h \to [0,1]$. By exploiting midpoint

quadrature, one obtains

$$\mathcal{D}^h(R^h,T^h;u^{h,j}) = \tilde{h}\frac{1}{2}\|T^h(\omega^h - u^{h,j}) - R^h\|_2^2$$

and $\mathcal{R}^h(u^{h,j}) = \tilde{h}\|\mathcal{B}^h u^{h,j}\|_2^2$, as a discrete analogue for (2) and (4), respectively; here, $\tilde{h} = \prod_{i=1}^d h^i$ (further details can e.g. be found in [Mod09]).

A semi-implicit discretisation of (15) reads

$$u^{h,j+1} = \left(E_{n_d} + h_t\alpha\mathcal{A}^h\right)^{-1}(u^{h,j} + b^{h,j}(\omega^h,T^h,R^h,u^{h,j})). \quad (16)$$

The force vector, $b^{h,j}$, in (16) is at this computed via

$$b^{h,j}(\omega^h,T^h,R^h,u^{h,j}) = -r\tilde{\nabla}^{h,d}T^h(\omega^h - u^{h,j}),$$

where $r = (R^h(\omega^h) - T^h(\omega^h - u^{h,j}))$ and $\tilde{\nabla}^{h,d}$ is a sparse matrix, which represents a central finite difference approximation of ∇. Likewise, we introduce the sparse matrices, $\nabla^{h,d}$ (backward differences), and, $\Delta^{h,d}$, to approximate the NABLA and LAPLACIAN operators within $\mathcal{A}^h$. The discrete representations of the individual differential operators, $\mathcal{A}^h$, are given by

$$\mathcal{A}^{D,h} = E_d \otimes \Delta^{h,d} \in \mathbf{R}^{n_d\times n_d},$$

$E_d = \mathrm{diag}(1,\dots,1) \in \mathbf{R}^{d\times d}$ and

$$\mathcal{A}^{C,h} = (\mathcal{A}^{D,h})^\mathsf{T}\mathcal{A}^{D,h} \in \mathbf{R}^{n_d\times n_d},$$

for diffusion and curvature regularisation, respectively. For elastic regularisation of 1st and 2nd order we have

$$\mathcal{A}^{E,h} = -\mu\Delta^{h,d} - (\lambda+\mu)\nabla^{h,d}(\nabla^{h,d})^\mathsf{T} \in \mathbf{R}^{n_d\times n_d}$$

and

$$\mathcal{A}^{E2,h} = \mu\Delta^{h,d}\Delta^{h,d} + (\lambda+2\mu)\Delta^{h,d}\nabla^{h,d}(\nabla^{h,d})^\mathsf{T} \in \mathbf{R}^{n_d\times n_d},$$

respectively.

3.3. Numerical Time Integration

A conventional approach would be to directly solve the SI, linear system (15) via iterative sparse matrix solvers. In case $\mathcal{R}_D$ is considered, the regularisation decouples along each spatial direction. Thus,

$$u^{h,j+1} = \left(E_{n_d} + h_t\alpha\textstyle\sum_{l=1}^d \mathcal{A}_l^{D,h}\right)^{-1}\tilde{u}^{h,j}, \quad (17)$$

where $\tilde{u}^{h,j} := (u^{h,j} + h_t b^{h,j}(\omega^h,T^h,R^h,u^{h,j}))$. This leads to the idea of additive operator splitting (AOS) [WRV98, Mod04, FM02], where the inverse in (17) is replaced by the sum of inverses. Thus, (17) becomes

$$u^{h,j+1} = \frac{1}{d}\sum_{l=1}^d \left(E_{n_d} + h_t\alpha\mathcal{A}_l^{D,h}\right)^{-1}\tilde{u}^{h,j}. \quad (18)$$

This considerably speeds up the numerical solution since AOS yields a tridiagonal system (each $\mathcal{A}_l^h$ is tridiagonal but $\sum_{l=1}^d \mathcal{A}_l^h$ in (17) is not), which can efficiently be solved by e.g. the tridiagonal matrix algorithm (TDMA). Other techniques, for efficiently solving (15), which are not considered in the present manuscript, are FOURIER [Mod04, CNH07, LRVMMS08] or multigrid [CTH05,Hen05,CC11,FSHW08] methods.

There is no doubt, that these techniques are fast, efficient and theoretically sound. However, they are quite elaborate, in particular when it comes to designing parallel algorithms. In addition, they are often tailored to a specific type of regulariser or might not necessarily allow for adaptive regularisation models [Kab06, CNH07, SRWHE12]. An alternative is to use explicit numerical time integration,

$$u^{h,j+1} = \left(E_{n_d} - h_t\alpha\mathcal{A}^h\right)u^{h,j} + h_t b^{h,j}(\omega^h,R^h,T^h,u^{h,j}), \quad (19)$$

which in turn does not demand the solution of a semi-linear system. However, it is well known from numerical analysis that explicit time integration is subject to a time step size restriction (CFL condition; cf. e.g. [Str04]). Considering (19), we have to adhere to

$$\rho\left(E_{n_d} - h_t\alpha\mathcal{A}^h\right) < 1 \quad\Rightarrow\quad h_t < \frac{2}{\alpha\rho(\mathcal{A}^h)} =: h_{t,\max}, \quad (20)$$

in order to guarantee convergence. Here,

$$\rho(M) := \max_i\{\lambda_i : \lambda_i \in \sigma(M), i = 1,\dots,n, n\in\mathbf{N}\}$$

is the spectral radius of any $M \in \mathbf{R}^{n\times n}$ with spectrum

$$\sigma(M) := \{\lambda_i : \lambda_i \text{ is an eigenvalue of } M\}.$$

However, there exist elegant strategies [Gen79, GS78, AAG96, GWB10] to stabilise (19). The basic idea is to relax the strong stability requirement in (20) by a cyclic variation of the size of a series of substeps, $h_{t,i}^\star$, $i = 0,\dots,w-1$, $w\in\mathbf{N}$, of a given exterior step, h_t. At this, stability is only demanded at the end of each cycle. The relaxed stability requirement reads

$$\rho\left(\textstyle\prod_{i=0}^{w-1}\left(E_{n_d} - h_{t,i}^\star\alpha\mathcal{A}^h\right)\right) < 1, \quad (21)$$

which is equivalent to $|\prod_{i=0}^{w-1}1 - h_{t,i}^\star\alpha\lambda| < 1 \;\; \forall\lambda\in\sigma(\mathcal{A}^h)$. With this, the computational rule for the cyclic, explicit time integration is given by

$$u^{h,j+1} = \hat{u}^{h,j} + h_t b^{h,j}(\omega^h,T^h,R^h,u^{h,j}). \quad (22)$$

where $\hat{u}^{h,j} := \prod_{i=0}^{w-1}\left(E_{n_d} - h_{t,i}^\star\alpha\mathcal{A}^h\right)u^{h,j}$. The implementation complexity for (22) is essentially the same as for (19). The gain in efficiency is due to the computational rule for the substeps, $h_{t,i}^\star$, up to half of which violate the stability requirement in (20) rendering (22) as efficient as (semi-)implicit methods.

The remaining question is, how to choose the substeps. In super-time-stepping [Gen79, GS78, AAG96] (STS) the computational rule for, $h_{t,i}^\star$, is determined explicitly. That is, one searches for an optimal set of time steps in the sense that the

duration (i.e. the exterior step), $h_t = \sum_{i=0}^{w-1} h^\star_{t,i}$, is maximised subject to the stability requirement

$$|\prod_{i=0}^{w-1}(1 - h^\star_{t,i}\alpha\lambda)| \leq \kappa \;\forall\lambda \in [\gamma, \lambda_{\max}],$$

$\gamma \in (0, \lambda_{\min}]$ and $\kappa \in (0,1)$, where $\lambda_{\min}$ and $\lambda_{\max}$ are the smallest and largest eigenvalues of $\mathcal{A}^h$. Relating this problem to the optimality properties of Chebychev polynomials yields [AAG96]

$$h^\star_{t,i,\mathrm{STS}} = h_{t,\max}\left((-1+\nu)\cos(\pi i/(w-1)) + 1 + \nu\right), \quad (23)$$

$i = 0, \ldots, w-1$, where, $\nu := \gamma/\lambda_{\max}$, $\nu \in (0, \lambda_{\min}/\lambda_{\max}]$.

Recently, a similar approach [GWB10] has been presented (denoted by EE* (**e**xplicit **E**uler)). In [GWB10] the connection between iterated box filtering (which is a stable operation) and conditionally stable, explicit numerical time integration of the diffusion equation, has been explored. In [GWB10] this connection is proven to exist. The computational rule for the substeps is given by [GWB10]

$$h^\star_{t,i,\mathrm{EE}^\star} = \frac{h_{t,\max}}{2\cos^2(\pi\frac{2i+1}{4w+2})}. \quad (24)$$

The final step before applying (23) or (24), is the computation of an estimate for $h_{t,\max}$. This is not a problem in practice, due to the existence of the *Gershgorin circle theorem* (cf. e.g. [GL96, theorem 7.2.1; p. 320]). This theorem provides a straightforward rule for estimating the spectral properties of $\mathcal{A}^h$ and by that—according to (21)—for estimating $h_{t,\max}$.

Under the assumption of exact arithmetic, the ordering of the individual time steps, $h^\star_{t,i}$, $i = 0, \ldots, w-1$, is of no relevance. In practice, exact arithmetic is not given. Round-off errors might accumulate during the computation and by that cause instabilities in case w becomes large. Therefore, it has been suggested to rearrange the time steps, $h^\star_{t,i}$, within so-called κ-cycles [Gen79, GS78]: Let the steps, $h^\star_{t,i}$, be collected in a w-tuple, $h^\star_t = (h^\star_{t,i}) \in \mathbf{R}^w$. The permutation of these entries, $h^\star_{t,i}$, is assigned to the w-tuple, $\tilde{h}^\star_t = (h^\star_{t,\phi(i)}) \in \mathbf{R}^w$, according to the heuristic rule $\phi(i) := (i+1)s \bmod p$. Here, $p \in \mathbf{N}$ is the next largest prime number, $p > w$, and $s > 0$ is a user defined parameter.

The regularisation parameter, α, can be relaxed during the computation (controlled by an iteration number n_α and the relaxation parameter β). Convergence is tested for according to (modified from [Mod09])

$$\begin{aligned}
&(c_1) \quad \mathcal{J}^{h,j} - \mathcal{J}^{h,j-1} < 0,\\
&(c_2) \quad |\mathcal{J}^{h,j} - \mathcal{J}^{h,j-1}| \leq \varepsilon_{\mathcal{J}}(1 + \mathcal{J}^{h,0}),\\
&(c_3) \quad \|u^{h,j} - u^{h,j-1}\|_2 \leq \varepsilon_u(1 + \|u^{h,j}\|_2),\\
&(c_4) \quad \|\delta\mathcal{J}^{h,j}\|_2 \leq \varepsilon_{\delta\mathcal{J}}(1 + \mathcal{J}^{h,0}),\\
&(c_5) \quad \|\delta\mathcal{J}^{h,j}\|_2 \leq 10^3\varepsilon,\\
&(c_6) \quad \alpha \leq \varepsilon_\alpha,\\
&(c_7) \quad j > n_j.
\end{aligned}$$

Figure 2: *Synthetic test data; from left to right: R^h, T^h, $1 - |R^h - T^h|$ and grid overlaid onto T^h.*

The iterations are stopped in case $(c_1) \vee ((c_2) \wedge (c_3) \wedge (c_4)) \vee (c_5) \vee (c_6) \vee (c_7)$. Here, $\varepsilon_{\mathcal{J}} > 0$, $\varepsilon_{\delta\mathcal{J}} > 0$, $\varepsilon_u > 0$ and $\varepsilon_\alpha > 0$ are user defined parameters and $\varepsilon > 0$ represents the machine precision. A multiresolution framework (based on [Mod09]) is used in order to speed up the computation. To solve the semi-implicit system, MATLAB's `mldivide` is used for the results included in this study. However, any other algorithm suitable for solving a sparse linear system can be applied (e.g. GMRES, KRYLOV subspace methods, multigrid,...).

4. Numerical Experiments

To test the discussed framework, numerical experiments in terms of a synthetic test problem are performed. As a reference data set, R^h, a MR brain template [CZK*98] is considered. R^h is deformed according to $y^h_r = \omega^h - 7(\sin(2\pi\nu\omega^h_1), \cos(2\pi\nu\omega^h_2))^\mathsf{T}$, where $\omega^h_i = (x^i_{1,\ldots,1}, \ldots, x^i_{m^1,m^2}) \in \mathbf{R}^{m^1 m^2}$, $i = 1,2$ and $\nu = 1.25 \cdot 10^{-2}$ and $T^h = R^h(y^h_r)$ (see Fig. 2 for an illustration; the visualisation is based on [Mod09]). It is possible to compute the relative error, $\delta u^h = \|u^h - u^h_{\mathrm{ref}}\|/\#u^h_{\mathrm{ref}}$, as well as a point-wise map, $e^h : \Omega^h \to \mathbf{R}$, of the L^2-distance between known and computed displacement vectors.

The regularisation parameter is set to $\alpha = 2.0$ (curvature), $\alpha = 0.2$ (diffusion), $\alpha = 0.2$ ($\mu = 1.0$, $\lambda = 0.0$, elastic) and $\alpha = 1.0$ ($\mu = 1.0$, $\lambda = 0.0$, 2^{nd} order elastic). The maximum number of iterations is set to $m_t = 800$. Further, $n_\alpha = m_t$, $\beta = 1$, $h_t = 1.0$, $\varepsilon_{\mathcal{J}} = 10^{-3}$, $\varepsilon_u = 5 \cdot 10^{-3}$, $\varepsilon_{\delta\mathcal{J}} = 5 \cdot 10^{-3}$ and $\varepsilon_\alpha = 10^{-5}$. The initial distance between T^h and R^h is $7.231 \cdot 10^2$. The results are displayed in Fig. 3 and summarised in Tab. 1. At this, values for the determinant of the JACOBIAN matrix, $J(y^h)$, are provided (computed via finite difference approximations). The strictly positive JACOBIANs suggest regular mappings (no folding). The error map, e^h, is computed for $\{x_k \in \Omega^h : R^h(x_k) > 0\}$ to not account for errors, where there is no information to drive the registration. In addition, plots that relate the convergence of standard semi-implicit and the proposed explicit methods are displayed in Fig. 4. As can be seen, the semi-implicit and the explicit solution strategy perform equivalent.

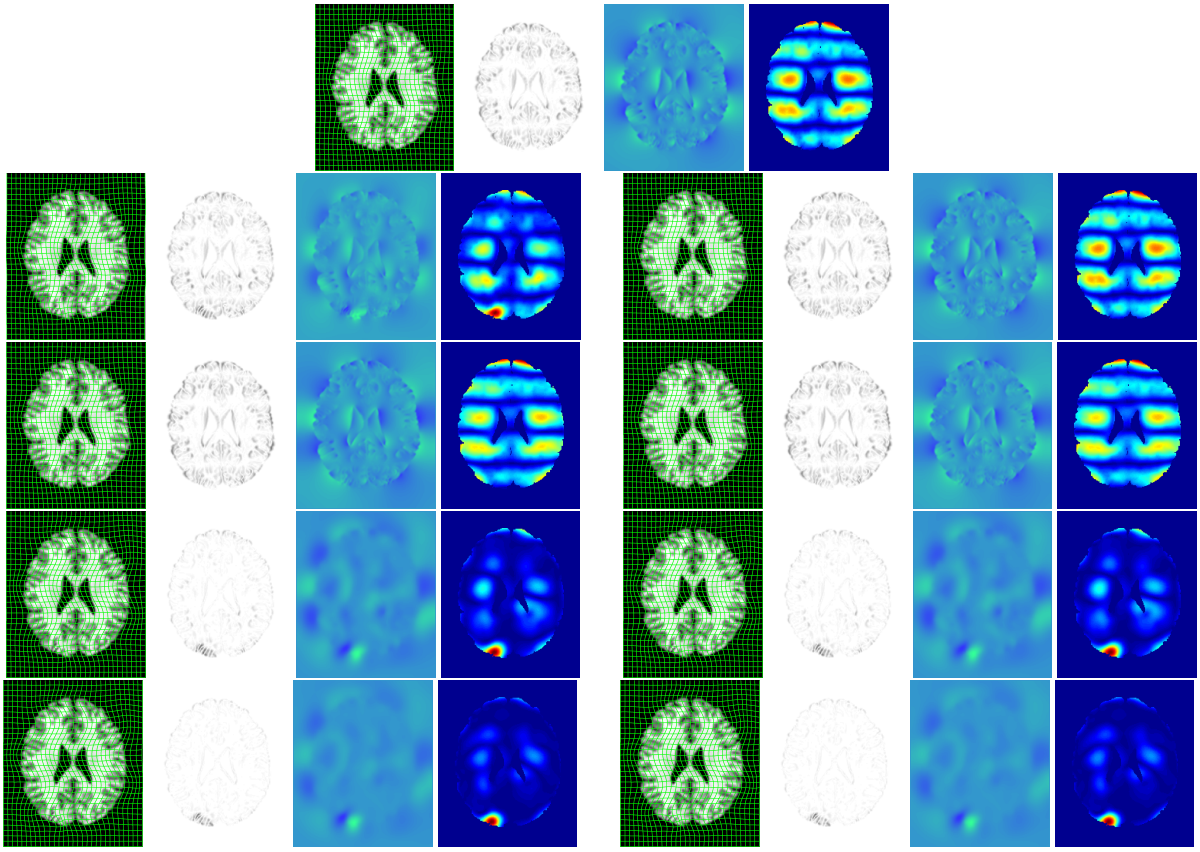

Figure 3: *Registration results. Each set of 4 images displays (from left to right) the deformed template image, $T^h(y^h)$, with a grid overlaid, $1-|R^h-T^h(y^h)|$, $J(y^h)$ and e^h. Each row provides results for a different regularisation model with respect to the individual numerical schemes (1st row: diffusion SI; 2nd row: diffusion AOS (left) and diffusion EE* (right); 3rd row: elastic SI (left) and elastic EE* (right); 4th row: curvature SI (left) curvature EE* (right); 5th row: 2^{nd} order elastic SI (left) and 2^{nd} order elastic EE* (right)).*

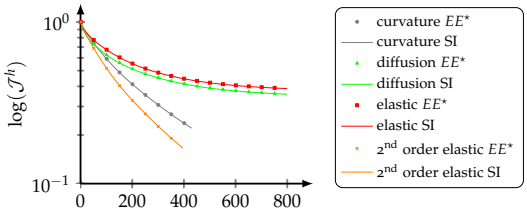

Figure 4: *Rate of convergence. Displayed is a semi-logarithmic plot of the objective value, $\mathcal{J}^h$, versus the iterations for the semi-implicit and explicit numerical strategies with respect to different regularisation models. The computation is performed only on the highest resolution level.*

5. Discussion and Conclusion

In the present manuscript an alternative numerical framework for variational non-rigid image registration based on cyclic numerical time integration has been discussed. This work aims at providing an efficient alternative to approximate convolution based registration models [BNG96, Thi98, VPPA08, VPPA09, CNH09, CNH10, BKF10]. These models have gained great popularity in recent years, due to their linear complexity and ease of implementation. However, they are less accurate than their counter parts in the OD framework based on numerical differentiation to solve the ELEs.

The fundamental aim of this work is to provide a framework that has a low implementation complexity and at the same time is efficient and shares the sound theoretical foundation of available techniques in the OD framework [CTH05, Hen05, CC11, FSHW08, Mod04, FM02, CNH07, LRVMMS08]. There is no doubt that these techniques provide efficient and sophisticated means for solving the considered PDE system. However, they might not always be applicable. That is, FOURIER-based approaches [Mod04, CNH07, LRVMMS08] cannot be used in case adaptive

Table 1: *Quantitative analysis of the registration results. Provided are the resulting distance, the resulting relative change in distance* $r = \mathcal{D}(R^h, T^h(y^h))/\mathcal{D}(R^h, T^h)$*, the range of the* JACOBIAN*,* $J(y^h)$*, the relative error,* δu^h*, as well as the maximum error for the* ℓ^2*-norm between ground truth and computed displacement field.*

		$\mathcal{D}(R^h, T^h(y^h))$	r	J^h	$\delta u^h/\mathrm{m}$	$\max(e^h)/\mathrm{m}$
$\mathcal{A}^{D,h}$	SI	$6.770 \cdot 10^{1}$	$9.362 \cdot 10^{-2}$	$[5.869 \cdot 10^{-1}, 1.400]$	$1.632 \cdot 10^{-3}$	$5.339 \cdot 10^{-3}$
	AOS	$5.474 \cdot 10^{1}$	$7.570 \cdot 10^{-2}$	$[3.252 \cdot 10^{-1}, 1.547]$	$1.622 \cdot 10^{-3}$	$6.980 \cdot 10^{-3}$
	EE*	$6.779 \cdot 10^{1}$	$9.374 \cdot 10^{-2}$	$[5.868 \cdot 10^{-1}, 1.400]$	$1.633 \cdot 10^{-3}$	$5.342 \cdot 10^{-3}$
$\mathcal{A}^{C,h}$	SI	$1.803 \cdot 10^{1}$	$2.493 \cdot 10^{-2}$	$[4.930 \cdot 10^{-1}, 1.545]$	$7.214 \cdot 10^{-4}$	$6.924 \cdot 10^{-3}$
	EE*	$1.826 \cdot 10^{1}$	$2.526 \cdot 10^{-2}$	$[4.955 \cdot 10^{-1}, 1.542]$	$7.312 \cdot 10^{-4}$	$6.897 \cdot 10^{-3}$
$\mathcal{A}^{E,h}$	SI	$7.672 \cdot 10^{1}$	$1.061 \cdot 10^{-1}$	$[7.322 \cdot 10^{-1}, 1.250]$	$1.548 \cdot 10^{-3}$	$5.245 \cdot 10^{-3}$
	EE*	$7.679 \cdot 10^{1}$	$1.062 \cdot 10^{-1}$	$[7.322 \cdot 10^{-1}, 1.250]$	$1.549 \cdot 10^{-3}$	$5.247 \cdot 10^{-3}$
$\mathcal{A}^{E2,h}$	SI	$1.065 \cdot 10^{1}$	$1.473 \cdot 10^{-2}$	$[2.977 \cdot 10^{-1}, 1.741]$	$5.404 \cdot 10^{-4}$	$8.688 \cdot 10^{-3}$
	EE*	$1.065 \cdot 10^{1}$	$1.473 \cdot 10^{-2}$	$[2.982 \cdot 10^{-1}, 1.741]$	$5.414 \cdot 10^{-4}$	$8.697 \cdot 10^{-3}$

regularisation [Kab06, CNH07, SRWHE12] is considered. AOS [Mod04, FM02] can only be applied if the matrix operator, $\mathcal{A}^h$, has a rich structure and decouples with respect to each spatial direction. Clearly, multigrid techniques [CTH05,Hen05,CC11,FSHW08] are generally applicable, feature linear complexity and have a high rate of convergence. However, their implementation is a rather delicate matter. The discussed framework is generally applicable, accurate, has the theoretical sound background of conventional approaches within the OD framework and features a low implementation complexity. It has been demonstrated experimentally that it performs equivalent to semi-implicit approaches. Generalisability has been demonstrated by testing the methodology within a generic framework for variational non-rigid image registration based on quadratic regularisation, accounting for diffusion [FM02], curvature [FM03], elastic [Bro81, Chr96] and 2$^{\text{nd}}$ order elastic [CNH10] regularisation.

However, this reduced implementation complexity does not come for free. A generic problem when considering explicit numerical time integration for solving the considered system of PDEs is that the solution establishes on a pointwise basis. Therefore, the effect of the regularisation is controlled locally and not globally. In the implicit case, the solution is available immediately throughout the entire domain, which makes these techniques—from a theoretical point of view—more suited for the considered problem. However, as has been demonstrated in the present manuscript, only marginal differences (qualitatively as well as quantitatively) are to be observed when comparing explicit and implicit implementations. A complete analysis and comparison to other approaches (such as multigrid [CTH05, Hen05, CC11, FSHW08], FOURIER [Mod04, CNH07, LRVMMS08] or convolution based techniques [BNG96, Thi98, VPPA08, VPPA09, CNH09, CNH10, BKF10]) remains subject to future work.

The present implementation is conceptual (for both–the implicit and the explicit implementation) and by that by no means optimised for speed, yet. As such, we did not provide a detailed analysis of computational performance. It is based on a sparse matrix-vector framework and implemented in MATLAB in order to demonstrate general applicability and keep track of the precise structure of the differential operators. Turning to parallel architectures as well as to matrix free implementations is expected to dramatically improve on the performance. This is something to be done in our future work, which also includes a detailed analysis of the runtime.

The intended application for the designed non-rigid registration framework is the analysis in serial or cross-population brain tumour imaging studies [MTS*12a, MTS*12b, HDB08, GBD11].

References

[AAG96] ALEXIADES V., AMIEZ G., GEREMAUD P.-A.: Super-time-stepping acceleration of explicit schemes for parabolic problems. *Com Num Meth Eng 12* (1996), 31–42. 2, 4, 5

[BKF10] BEUTHIEN B., KAMEN A., FISCHER B.: Recursive Green's function registration. In *Med Image Comput Comput Assist Interv* (2010), pp. 546–553. 2, 6, 7

[BNG96] BRO-NIELSEN M., GRAMKOW C.: Fast fluid registration of medical images. In *Proc Vis Biomed Comput* (1996), pp. 267–276. 1, 2, 6, 7

[Bro81] BROIT C.: *Optimal registration of deformed images*. PhD thesis, Computer and Information Science, University of Pennsylvania, 1981. 1, 2, 3, 7

[CC11] CHUMCHOB N., CHEN K.: A robust multigrid approach for variational image registration models. *J Comp Appl Math 236*, 5 (2011), 653–674. 1, 2, 4, 6, 7

[CHH04] CRUM W. R., HARTKENS T., HILL D. L. G.: Non-rigid image registration: theory and practice. *Brit J Radiol 77*, 2 (2004), S140–S153. 1

[Chr96] CHRISTENSEN G. E.: *Deformable Shape Models for Anatomy*. PhD thesis, Sever Institute of Technology, Washington University, 1996. 1, 2, 3, 7

[CNH07] CAHILL N. D., NOBLE J. A., HAWKES D. J.: Fourier methods for nonparametric image registration. In *Proc IEEE CVPR* (2007), pp. 1–8. 2, 4, 6, 7

[CNH09] CAHILL N. D., NOBLE J. A., HAWKES D. J.: A demons algorithm for image registration with locally adaptive regularization. In *Med Image Comput Comput Assist Interv* (2009), pp. 574–581. 2, 6, 7

[CNH10] CAHILL N., NOBLE J. A., HAWKES D. J.: Extending the quadratic taxonomy of regularizers for nonparametric registration. In *SPIE Medical Imaging: Image Processing* (2010), vol. 7623, pp. 76230B–1–76230B–12. 2, 3, 6, 7

[CRM96] CHRISTENSEN G. E., RABBIT R., MILLER M.: Deformable templates using large deformation kinematics. *IEEE Trans Imag Proc 5*, 10 (1996), 1435–1447. 2

[CTH05] CRUM W. R., TANNER C., HAWKES D. J.: Multiresolution anisotropic fluid registration: Evaluation in magnetic resonance breast imaging. *Phys Med Biol 50*, 21 (2005), 5153–5174. 1, 2, 4, 6, 7

[CZK*98] COLLINS D. L., ZIJDENBOS A. P., KOLLOKIAN V., SLED J. G., KABANI B. J., HOLMES C. J., EVANS A. C.: Design and construction of a realistic digital brain phantom. *IEEE Trans Med Imaging 17*, 3 (1998), 463–468. 5

[DHLH11] DARKNER S., HANSEN M. S., LARSEN R., HANSEN M. F.: Efficient hyperelastic regularization for registration. In *Image Analysis* (2011), vol. LNCS 6688, pp. 295–305. 1, 2

[FM02] FISCHER B., MODERSITZKI J.: Fast diffusion registration. *AMS Contemporary Mathematics, Inverse Problems, Image Analysis, and Medical Imaging 313* (2002), 117–129. 1, 2, 3, 4, 6, 7

[FM03] FISCHER B., MODERSITZKI J.: Curvature based image registration. *J Math Imag Vis 18*, 1 (2003), 81–85. 1, 2, 3, 7

[FM08] FISCHER B., MODERSITZKI J.: Ill-posed medicine–an introduction into image registration. *Inv Prob 24*, 3 (2008), 034008. 1, 2

[FSHW08] FROHN-SCHAUF C., HENN S., WITSCH K.: Multigrid based total variation image registration. *Comput Visual Sci 11*, 2 (2008), 101–113. 2, 4, 6, 7

[GBD11] GOOYA A., BIROS G., DAVATZIKOS C.: Deformable registration of glioma images using EM algorithm and diffusion reaction modeling. *IEEE Trans Med Imaging 30*, 2 (2011), 375–390. 7

[Gen79] GENTZSCH W.: Numerical solution of linear and nonlinear parabolic differential equations by a time-descritsation of third order accuracy. In *Proceedings of the 3rd GAMM-Conference on Numerical Methods in Fluid Mechanics* (1979), pp. 109–117. 2, 4, 5

[GL96] GOLUB G. H., LOAN C. F. V.: *Matrix Computations*, 3 ed. Johns Hopkins University Press, Baltimore, Maryland, US, 1996. 5

[GS78] GENTZSCH W., SCHLUTER A.: Über ein Einschrittverfahren mit zyklischer Schrittweitenänderung zur Lösung parabolischer Differentialgleichungen. *Z Angew Math Mech 58* (1978), T415–T416. 2, 4, 5

[GWB10] GREWENIG S., WEICKERT J., BRUHN A.: From box filtering to fast explicit diffusion. In *Pattern Recognition* (2010), vol. LNCS 6376, pp. 533–542. 2, 4, 5

[HDB08] HOGEA C., DAVATZIKOS C., BIROS G.: Brain-tumor interaction biophysical models for medical image registration. *SIAM J Sci Comput 30*, 6 (2008), 3050–3072. 7

[Hen05] HENN S.: A multigrid method for a fourth-order diffusion equation with application to image processing. *SIAM J Sci Comput 27*, 3 (2005), 831–849. 1, 2, 4, 6, 7

[HHH01] HAJNAL J. V., HILL D. L. G., HAWKES D. J. (Eds.): *Medical Image Registration*. CRC Press, Boca Raton, Florida, US, 2001. 1, 2

[HM04] HABER E., MODERSITZKI J.: Numerical methods for volume preserving image registration. *Inv Prob 20* (2004), 1621–1638. 2

[Kab06] KABUS S.: *Multiple-Material Variational Image Registration*. PhD thesis, University of Lübeck, Institute of Mathematics, 2006. 4, 7

[LRVMMS08] LARREY-RUIZ J., VERDÚ-MONEDERO R., MORALES-SÁNCHEZ J.: A fourier domain framework for variational image registration. *J Math Imag Vis 32*, 1 (2008), 57–72. 2, 4, 6, 7

[Mod04] MODERSITZKI J.: *Numerical methods for image registration*. Oxford University Press, New York, New York, US, 2004. 1, 2, 3, 4, 6, 7

[Mod09] MODERSITZKI J.: *FAIR: Flexible algorithms for image registration*. SIAM, Philadelphia, Pennsylvenia, US, 2009. 2, 4, 5

[MTS*12a] MANG A., TOMA A., SCHUETZ T. A., BECKER S., BUZUG T. M.: A generic framework for modeling brain deformation as a constrained parametric optimization problem to aid non-diffeomorphic image registration in brain tumor imaging. *Meth Inf Med* (2012). in press. 7

[MTS*12b] MANG A., TOMA A., SCHUETZ T. A., BECKER S., ECKEY T., MOHR C., PETERSEN D., BUZUG T. M.: Biophysical modeling of brain tumor progression: From unconditionally stable explicit time integration to an inverse problem with parabolic pde constraints for model calibration. *Med Phys 39*, 7 (2012), 4444–4460. accepted. 7

[PMS10] PÖSCHL C., MODERSITZKI J., SCHERZER O.: A variational setting for volume constrained image registration. *Inv Prob Imag 4*, 3 (2010), 505–522. 2

[SP12] SOTIRAS A., PARAGIOS N.: *Deformable Image Registration: A Survey*. Tech. Rep. RR-7919, Center for Visual Computing, Department of Applied Mathematics, Ecole Centrale de Paris, 2012. 1

[SRWHE12] SCHMIDT-RICHBERG A., WERNER R., HANDELS H., EHRHARDT J.: Estimation of slipping organ motion by registration with direction-dependent regularization. *Med Imag Anal 16* (2012), 150–159. 4, 7

[Str04] STRIKWERDA J. C.: *Finite Difference Schemes and Partial Differential Equations*. SIAM, Philadelphia, Pennsylvenia, US, 2004. 4

[Thi98] THIRION J.-P.: Image matching as a diffusion process: an analogy with maxwell's demons. *Med Imag Anal 2*, 3 (1998), 243–260. 1, 2, 6, 7

[VPPA08] VERCAUTEREN T., PENNEC X., PERCHANT A., AYACHE N.: Symmetric log-domain diffeomorphic registration: a demons-based approach. In *Med Image Comput Comput Assist Interv* (2008), pp. 754–761. 2, 6, 7

[VPPA09] VERCAUTEREN T., PENNEC X., PERCHANT A., AYACHE N.: Diffeomorphic demons: Efficient non-parametric image registration. *NeuroImage 45*, 1 (2009), S61–72. 2, 6, 7

[WRV98] WEICKERT J., ROMENY B. H., VIERGEVER M. A.: Efficient and reliable schemes for nonlinear diffusion filtering. *IEEE Trans Image Proc 7*, 3 (1998), 398–410. 4